Desalination and Water Treatment
www.deswater.com

doi: 10.1080/19443994.2013.781964

51 (2013) 7710–7720
December

Taylor & Francis
Taylor & Francis Group

Cd (II) removal by marine *Arthrobacter protophormiae* biomass: mechanism characterization and adsorption performance

Xue Song Wang

Department of Chemical Engineering, Huaihai Institute of Technology, Lianyungang, Jiangsu 222005, P.R. China
Tel. +86 518 85895408; Fax: +86 518 85895409; email: snowpine1969@126.com
Jiangsu Key Laboratory of Marine Biotechnology, Huaihai Institute of Technology, Lianyungang, Jiangsu 222005, P.R. China

Received 10 October 2012; Accepted 25 February 2013

ABSTRACT

Biomass of *Arthrobacter protophormiae* was used to remove Cd (II) from aqueous solution. The interaction of Cd (II) with *A. protophormiae* biomass was investigated by environmental scanning electron microscopy coupled with energy dispersive X-ray analysis and FTIR spectroscopy. Atomic force microscopy (AFM) used in the tapping mode elucidated the morphological changes in bacterial cells following Cd (II) binding. Adsorption of Cd (II) by biomass was investigated to quantify adsorption kinetics, adsorption capacity, and the effect of solution pH. The applicability of the Langmuir and Freundlich models was tested. The maximum adsorption capacity was found to be 31 mg/g for Cd (II) at 25°C. The adsorption process was found to follow the pseudo-first-order equation. The involvement of cellular phosphate and carboxyl groups in Cd (II) binding was ascertained by FTIR spectroscopy. Results indicate that a chemical interaction could be involved in Cd (II) sequestration by this bacterium. AFM analysis revealed that adsorption of Cd (II) onto biomass induced substantial modification on cell surfaces.

Keywords: Arthrobacter protophormiae; Cd (II); AFM; Sequestration; Characterization

1. Introduction

Contamination of the aqueous environments by heavy metals is a worldwide environmental problem due to their toxic effects and accumulation through the food chain. Among the heavy metals of public concern, cadmium has received much attention, probably due to its high toxicity. The harmful effects of cadmium include a number of acute and chronic disorders, such as "itai-itai" disease, renal damage, emphysema, hypertension, and testicular atrophy [1]. The main anthropogenic pathway through which cadmium enters the environment is via wastes from industrial processes such as electroplating, smelting, alloy manufacturing, pigments, plastic, cadmium-nickel batteries, fertilizers, pesticides, mining, pigments and dyes, textile operations, and refining [2].

Much effort has been made to develop physicochemical processes for cadmium removal. Major processes currently being suggested or employed for the removal of heavy metals, particularly cadmium, from wastewaters include precipitation [3], cementation [4],

Table 1
Microbial biomass used for Cd (II) removal

Microbial species	pH	Temp. (°C)	Uptake (mg/g)	References
Bacillus circulans	7	30	26.5	[12]
Enterobacter sp. J1	6	25	46.2	[13]
Pseudomonas putida	6	NA[a]	8	[14]
Streptomyces pimorina	5	NA[a]	30.4	[15]

[a]Not available.

ion exchange [5], membrane separation [6], solvent extraction [7], adsorption [8,9]. A detailed discussion on the advantages and disadvantages of all processes is presented by Rao et al. [2].

Recent attention has concentrated on biotechnological potential in metal removal processes [10]. Bacterial biomass represents an efficient and potential class of biosorbents for the removal of metal ions [11]. Several microbial biomasses have been investigated to remove Cd (II) from aqueous solutions and promising results obtained (Table 1).

The *Arthrobacter protophormiae* strain used was isolated from marine sediment and applied to remove Cd (II) from aqueous solutions. The objectives of this study were to (1) quantify adsorption kinetics, adsorption capacity, and the effect of solution pH; (2) elucidate the mechanism of Cd (II)–bacteria interaction by employing several analytical techniques such as FTIR spectroscopy, scanning electron microscopy/energy dispersive X-ray analysis (ESEM-EDX), and atomic force microscopy (AFM).

2. Materials and methods

Chemical reagents used in this study include: Cd $(NO_3)_2{\cdot}4H_2O$ (AR, Fu chen, Shanghai), HNO_3 (GR, Fu chen, Shanghai), NaOH (GR, Fu chen, Shanghai) and KNO_3 (AR, Fu chen, Shanghai). Deionized water from a Hydro-Service reverse osmosis/ion-exchange system (Model 2PRO-20) was used in all experiments.

2.1. Preparation of biomass

The *A. protophormiae* strain (G+) (characterized by 16S rDNA technology) used was isolated from marine sediment. Inocula from fresh slant were used to initiate preculture at 25°C. At the late logarithmic phase of growth, inocula of 1 mL were transferred and allowed to grow in 50 mL volume of the growth-culture medium which contained beef extract (1 kg/m^3), peptone (5 kg/m^3), and pH 7.6–7.8. For agar plates, 15 g of agar per liter was added before autoclaving.

The cells from the late exponential growth phase were harvested by centrifugation (10,000 × g, 10 min) at room temperature and washed three times with deionized water in the absence of metabolizable substrate. The biomass was freeze-dried for use.

2.2. Determination of point of zero charge

The point of zero charge (pH_{PZC}) of the biomass was determined by the solid addition method [16]. To a series of 100-mL conical flasks, 45 mL of KNO_3 solution of known strength was transferred. The pH_0 values of the solution were roughly adjusted from 2 to 12 by adding either 0.1 mol/L HNO_3 or NaOH. The total volume of the solution in each flask was made exactly to 50 mL by adding the KNO_3 solution of the same strength. The pH of the solutions was then accurately noted, and 0.1 g of biomass was added to each flask, which were securely capped immediately. The suspensions were then manually shaken and allowed to equilibrate for 48 h with intermittent manual shaking. The pH values of the supernatant liquid were noted. The difference between the initial (pH_0) and final pH (pH_f) values ($pH_0 - pH_f$) was plotted against the pH_0. The point of intersection of the resulting curve at that pH gave the pHzpc. The procedure was repeated for different concentrations (0.01, 0.1 mol/L) of KNO_3.

2.3. Characterization by ESEM-EDX, FTIR, and AFM

Cd-free control and Cd-loaded biomass were used for EDX microanalysis using a QUANTAX microanalytical system (Bruker, Germany) attached with FEI Quanta 250 environmental scanning electron microscope (USA) (ESEM-EDX). Cd-free control and Cd-loaded biomass were used for FTIR spectroscopic analysis. The infrared spectra were recorded within the range 400–4,000 cm^{-1} in a Tensor 27 FTIR Spectrometer (Bruke, Germany).

A Dimension ICON atomic force microscope (AFM, Bruker, Germany) was used to record AFM images. Cells were imaged using Silicon nitride (Si_3N_4) cantilevers (OTESPA, Bruker) with a spring constant of 70 N/m at a scan speed of 300 kHz in air. AFM imaging was performed using the tapping mode, where the tip makes intermittent contact with the sample as the tip is oscillated near its resonance frequency. The advantages of the tapping mode are that the sample is less likely to be damaged by the tip and that lateral forces are greatly reduced. Despite these advantages, there are very few reports on the application of this technique in investigating bacterial metal sequestration processes [17].

2.4. Adsorption experiments

The stock solution (1 kg/m^3) was prepared by dissolving a known quantity of cadmium nitrate (Cd $(NO_3)_2{\cdot}4H_2O$) in deionized water. The pH was adjusted with HNO_3 or NaOH using a PHS-3C pH meter (Jiangsu Jiangfen Instrumental Factory, China) using a combined glass electrode calibrated with buffers of pH 2, 4, and 7.

For each isotherm, a series of flasks were prepared with known volumes of serial dilutions of standardized metal salt solutions (0.02–0.1 kg/m^3). Weighed quantities of the dried biomass (5 kg/m^3) were added and the flasks were agitated at 150 rpm at 25˚C. The biomass was removed by centrifugation and the supernatant was analyzed for metal concentrations.

Kinetic studies were carried out with an initial concentration of 0.01 kg/m^3 and an adsorbent concentration of 5 kg/m^3 at 25˚C. After shaking, the solution samples were withdrawn at suitable time intervals.

The effect of pH on the Cd (II) adsorption was studied by varying the initial solution pH values (1–6.5) with an initial metal ion concentration of 0.01 kg/m^3. Temperature control was provided by the water bath shaker unit.

Dissolved Cd concentrations in acidified samples were measured using atomic absorption spectrophotometry (AAS, Beijing Puxi Scientific Instrumental Factory, China).

All glassware were washed with 1 mol/L HNO_3 and rinsed thoroughly with deionized water prior to use. All experiments were performed in triplicate and the mean values were used for data analyses. Controls were comprised of adsorbent in deionized water blank and adsorbent-free metal ions solutions.

2.5. Data analysis

The amount of metal ions sorbed by the biomass (q_e, mg/g) was calculated as follows:

$$q_e = \frac{V(C_0 - C_e)}{m} \quad (1)$$

where V is the solution volume (L), m is the amount of sorbent (g), and C_0 and C_e (mg/L) are the initial and equilibrium metal concentrations, respectively.

The removal efficiency (%) was calculated in the following

$$\text{Removal}\ (\%) = 100 \times \frac{C_0 - C_e}{C_0} \quad (2)$$

3. Results and discussion

3.1. Effect of solution pH

The percentage of Cd (II) removal was small at low pH values and increased as the pH increased (Fig. 1). Cadmium removal was less than 5% at pH 1 and rapidly increased to around 55% at pH 3.0. This behaviour is similar to copper removal by marine *Bacillus* sp. biomass [16].

The solution pH influences metal ion uptake by its effect on the charge of the sorbing aqueous metal ion species and on the surface charge of the biomass [18]. The Medusa computer program software developed by the Sweden Royal Institute of Technology was used for speciation analysis. At acidic media, the dominant species of Cd (II) are charged positively, Cd^{2+} (Fig. 2).

The pH_{PZC} of the biomass was determined to be 2.8 (Fig. 3), which is identical to the ZPC of the cell wall of a gram-positive bacterium [19]. At solution $pH > pH_{PZC}$, negatively charged sites predominate on the surface of biomass and thus favor the Cd (II) adsorption.

In gram-positive bacteria, the carboxylate and phosphate groups are primarily associated with the peptidoglycan; the peptidoglycan backbone is rich in carboxylate groups, and the associated teichoic acids are rich in phosphate groups [19]. The carboxylate (pKa 4.8) and phosphate groups (pKa1 2.12) carry negative charges that allow the cells to be potent scavengers of cations.

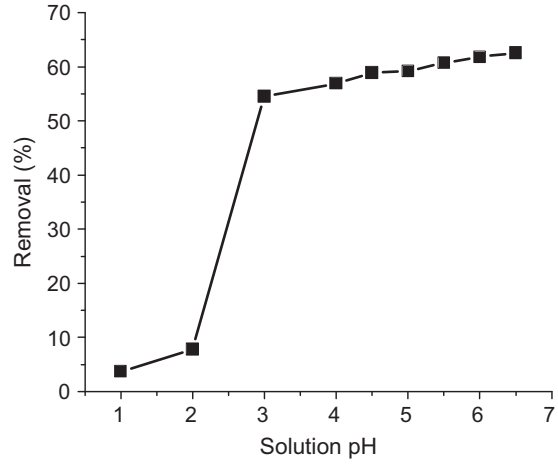

Fig. 1. Cd (II) adsorption by *A. protophormiae* biomass as a function of pH (Cd (II) initial concentration: 10 mg/L, adsorbent concentration: 5 g/L, reaction temperature: 25˚C, contact time 2 h).

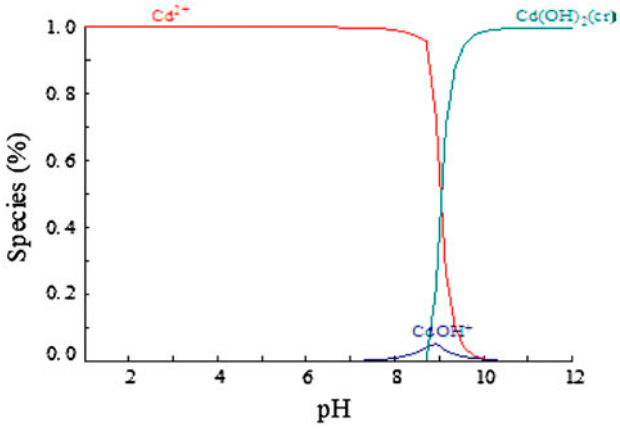

Fig. 2. Species fraction diagrams vs. pH (10 mg/L cadmium nitrate).

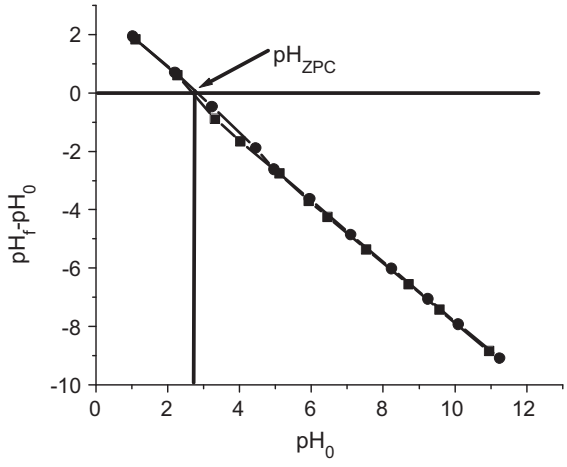

Fig. 3. Net surface charge of *A. protophormiae* biomass as a function of initial solution pH.

3.2. Effect of contact time

The Cd (II) reaction with *A. protophormiae* biomass was rapid, and more than 65% of Cd (II) was sequestered from the solution at pH 7 within the first 0.5 h (Fig. 4). The initial rapid adsorption gave way to a relatively slow rate of approaching to the equilibrium and saturation was reached after ca. 8 h. Based on these results, an 8-h contact time was used for the subsequent experiments.

To analyze the adsorption kinetics, the pseudo-first-order equation (Eq. (3)) and pseudo-second-order equation (Eq. (4)) [20] were applied to the experimental data. Both equations are expressed as

$$q_t = q_e[1 - \exp(1 - k_1 t)] \quad (3)$$

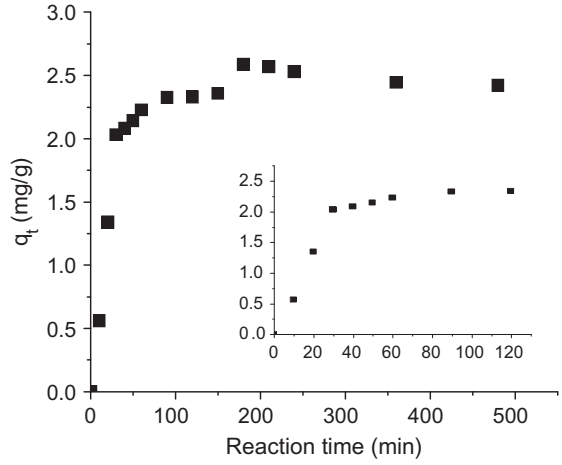

Fig. 4. Kinetics of Cd (II) adsorption by *A. protophormiae* biomass (pH 7, reaction temperature: 25°C, Cd (II) initial concentration: 10 mg/L, adsorbent concentration: 5 kg/m^3). The inset shows the q_t vs. reaction time at <120 min.

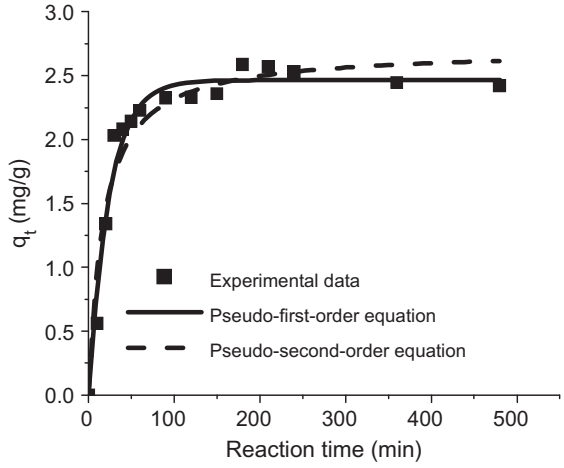

Fig. 5. Kinetic fittings by pseudo-first-order equation and pseudo-second-order equation, respectively

$$q_t = \frac{k_2 q_e^2 t}{1 + q_e k_2 t} \quad (4)$$

where q_e and q_t (mg/g) are the amounts of adsorbed adsorbate onto the adsorbent at equilibrium and at time t (h), respectively, k_1 (1/min) and k_2 (g/(mg min)) are the rate constants of pseudo-first-order equation and pseudo-second-order equation, respectively. Nonlinear regressions using a least-squares fitting program (Origin 7.0, OriginLab Corp., Northampton, MA) were conducted to acquire the best estimate of all constants.

Table 2
Fitting results of pseudo-second-order equation

	Pseudo-first-order equation			Pseudo-second-order equation		
	q_e (mg/g)	k_1 (1/min)	R^2	q_e (mg/g)	k_2 (g/(mg min)	R^2
Cd (II)	2.46	0.04	0.9724	2.7	0.022	0.9458

The fitting results are shown in Fig. 5 and related parameters acquired are summarized in Table 2. The value of q_e (2.46 mg/g) obtained by fitting using pseudo-first-order equation is close to the experimental value (2.44 mg/g). Moreover, the higher correlation coefficients (R^2) of pseudo-first-order equation implied that the kinetic data conformed to the pseudo-first-order equation [20].

3.3. Adsorption isotherm

The most commonly used equations (i.e. Langmuir (Eq. (5)) and Freundlich (Eq. (6) isotherms) were applied to the isothermal data. These two equations are generally written as

$$q_e = \frac{q_m b C_e}{1 + b C_e} \tag{5}$$

$$q_e = K_f C_e^{1/n} \tag{6}$$

where q_m is the maximum uptake (mg/g), b is the Langmuir constant (L/mg), K_f ([(mg/g)/(mg/L)$^{1/n}$]) and n (dimensionless) are the Freundlich empirical constants. Nonlinear regressions using a least-squares fitting program (Origin 7.0, OriginLab Corp., Northampton, MA) were conducted to acquire the best estimate of all constants.

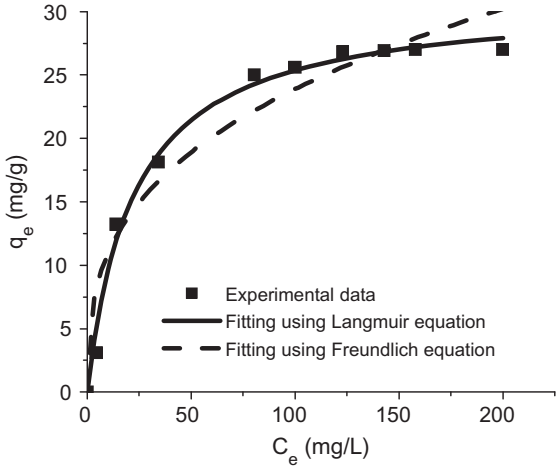

Fig. 6. Cd (II) adsorption isotherm on *A. protophormiae* biomass with the results fitted to the Langmuir and Freundlich isotherms (Contact time 8 h, pH 7, reaction temperature 25°C, adsorbent concentration 5 kg/m^3).

Cd (II) isotherm for *A. protophormiae* biomass and fitting results are shown in Fig. 6 and Table 3. The Freundlich adsorption isotherm is an indication of surface heterogeneity of the adsorbent while the Langmuir isotherm assumes that adsorption occurs in a monolayer, or it may only occur at a fixed number of localized sites on a surface on which all adsorption sites are identical and energetically equivalent. The higher correlation coefficient (R^2) for the Langmuir isotherm indicated that the equation adequately described the experimental data of the adsorption of Cd (II). The theoretical maximum uptake capacity (q_m) for Cd (II) of *A. protophormiae* biomass at 25°C was 31 mg/g and is comparable to those reported in Table 1.

3.4. FTIR analyses

Fig. 7(a) shows the FTIR spectra of Cd-free *A. protophormiae* biomass. The FTIR spectra clearly demonstrate that different functional groups are present on the biomass. The large band around 3,280 cm^{-1} was attributed to the stretching vibration of –OH of carboxylic acid [21]. In the range of 3,000–2,800 cm^{-1},

Table 3
Isotherm parameters of Cd (II) for *A. protophormiae* biomass

	Langmuir			Freundlich		
	q_m (mg/g)	b (L/mg)	R^2	K_f [(mg/g)/(mg/L)$^{1/n}$]	n (–)	R^2
Cd (II)	31	0.04	0.9916	5.03	2.95	0.9451

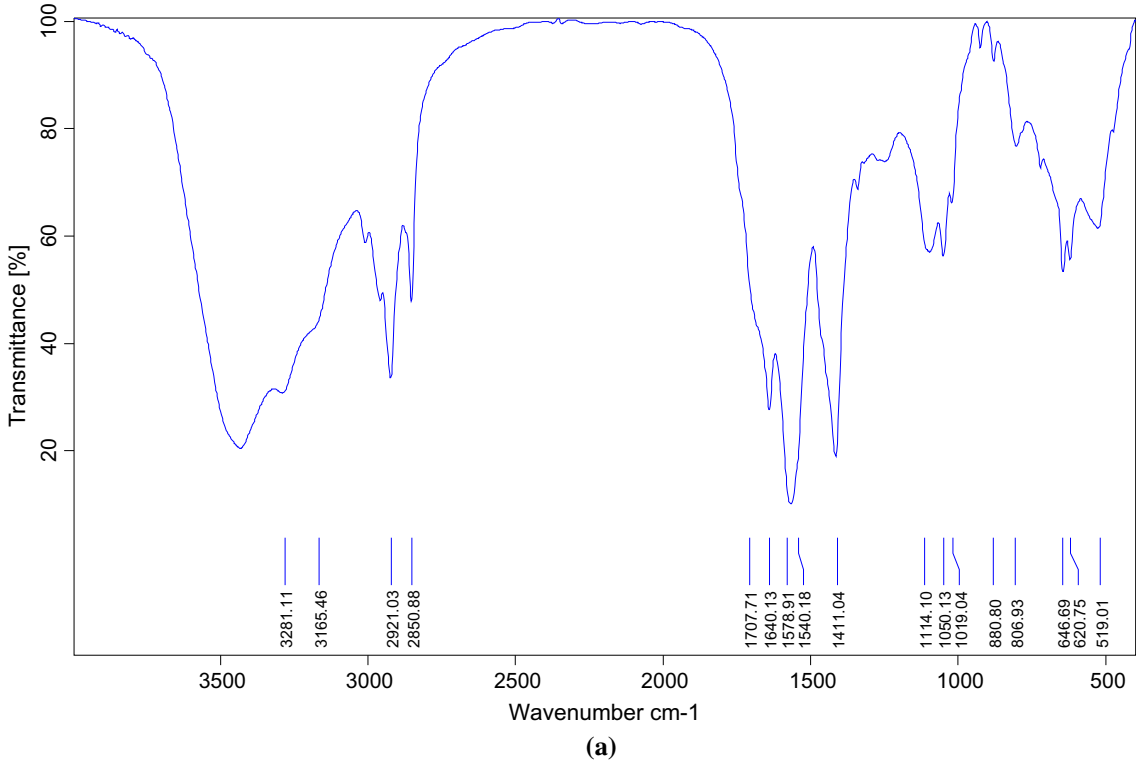

(a)

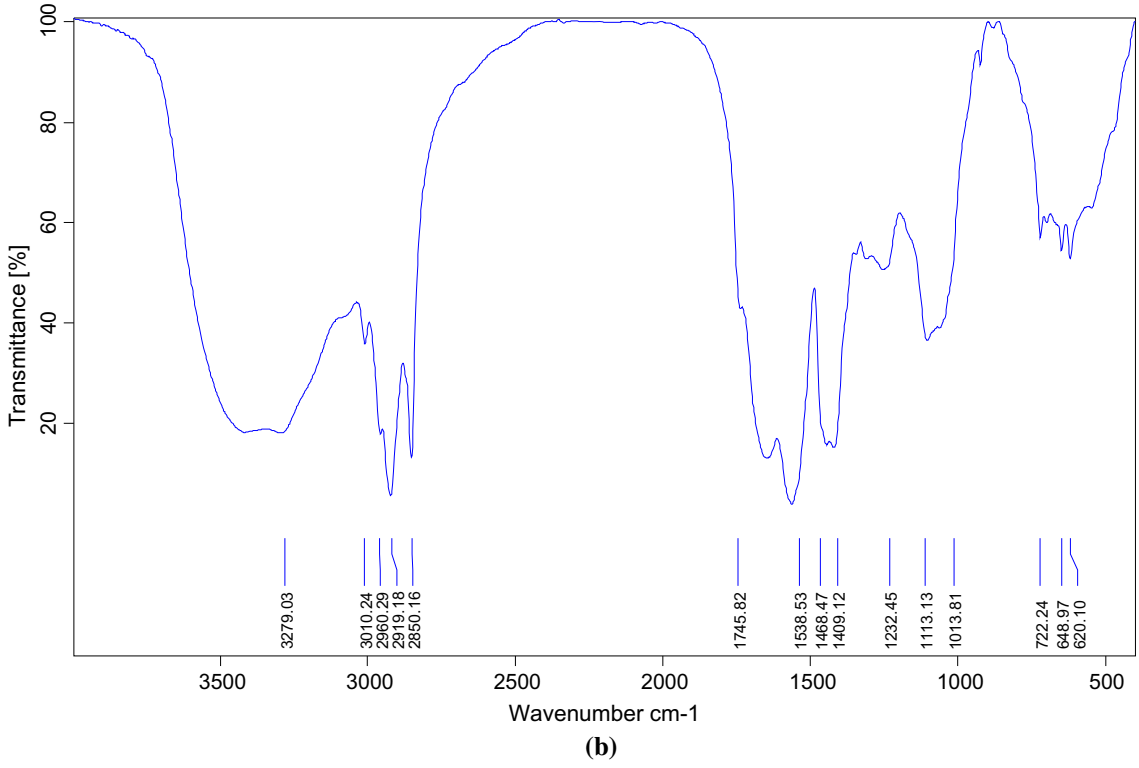

(b)

Fig. 7. FTIR spectra of Cd-free *A. protophormiae* (a) and Cd (II)-loaded *A. protophormiae* biomass (b).

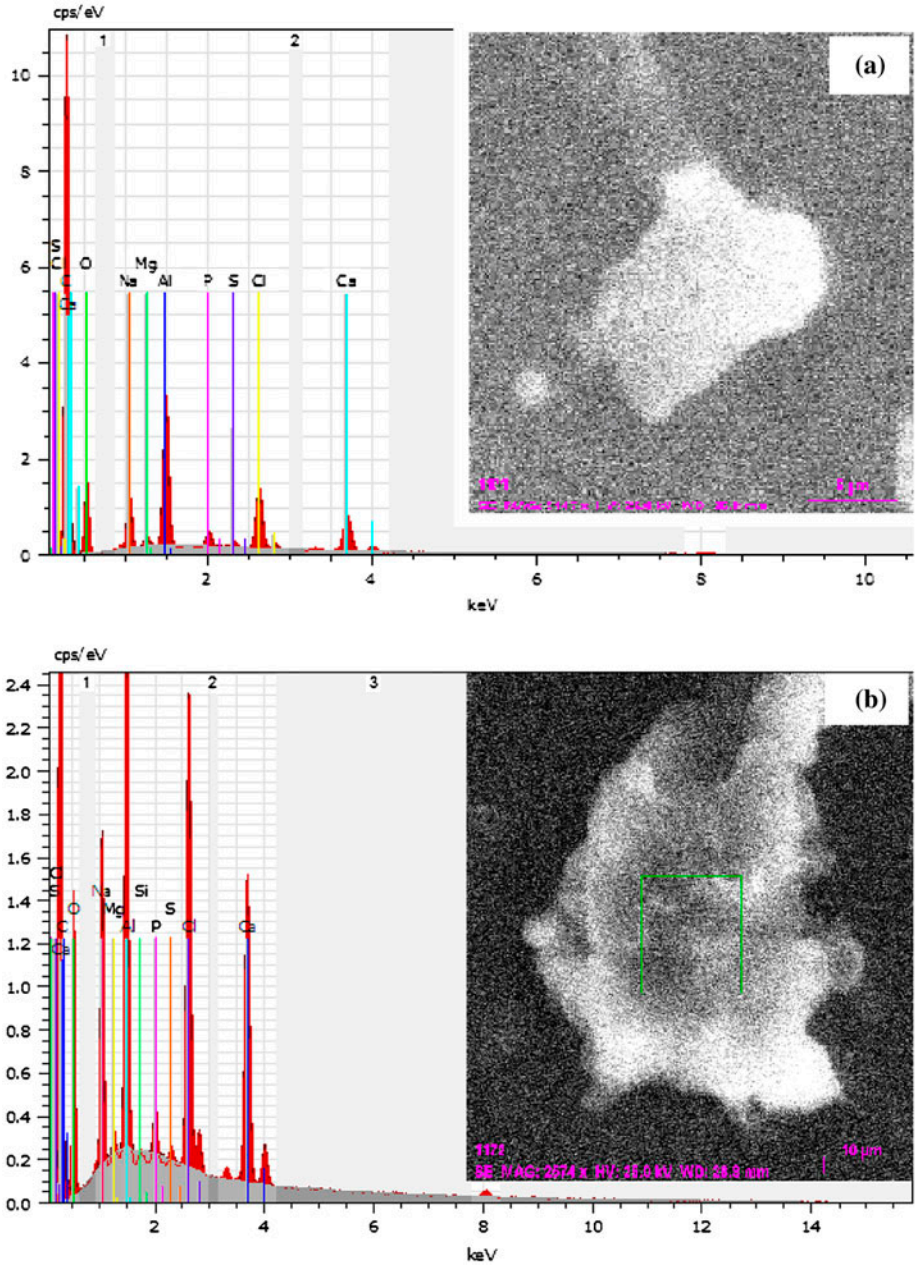

Fig. 8. SEM and EDS spectra of the biomass ((a) and (b): raw *A. protophormiae* biomass; (c) and (d): Cd (II)-loaded *A. protophormiae* biomass).

the bands are representative of symmetric and asymmetric vibrations of stretching of $-CH_3$ and $-CH_2$ groups. A peak observed at 1,707 cm^{-1} was attributed to carbonyl strething in carboxylate groups or ester groups [22]. A band located around 1,640 cm^{-1} may correspond to the superimposition of a different Amide Iband and a peak around 1,540 cm^{-1} corresponds to Amide II band [21–23]. Around 1,411 $cm^{-1,}$ $-CH_2$ bending vibration was observed. The peak around 1,114 cm^{-1} corresponds to the vibrations of C–O–P and/or P–O–P groups and the band around 1,050 cm^{-1} corresponds to the C–O and/or C–O–C from polysaccharides [22].

The Cd (II) adsorption induced some small modifications in the IR spectra (Fig. 7(b)). The neo-formed absorption peaks at 1,409 cm^{-1} and 1,232 cm^{-1} were confidently assigned to the presence of both carboxylate anions and phosphate/phosphoryl functional groups [9,22], indicating chemical interactions of Cd (II) with these groups.

The overall spectral analysis strongly supports the major role of carboxyl and phosphate/phosphoryl

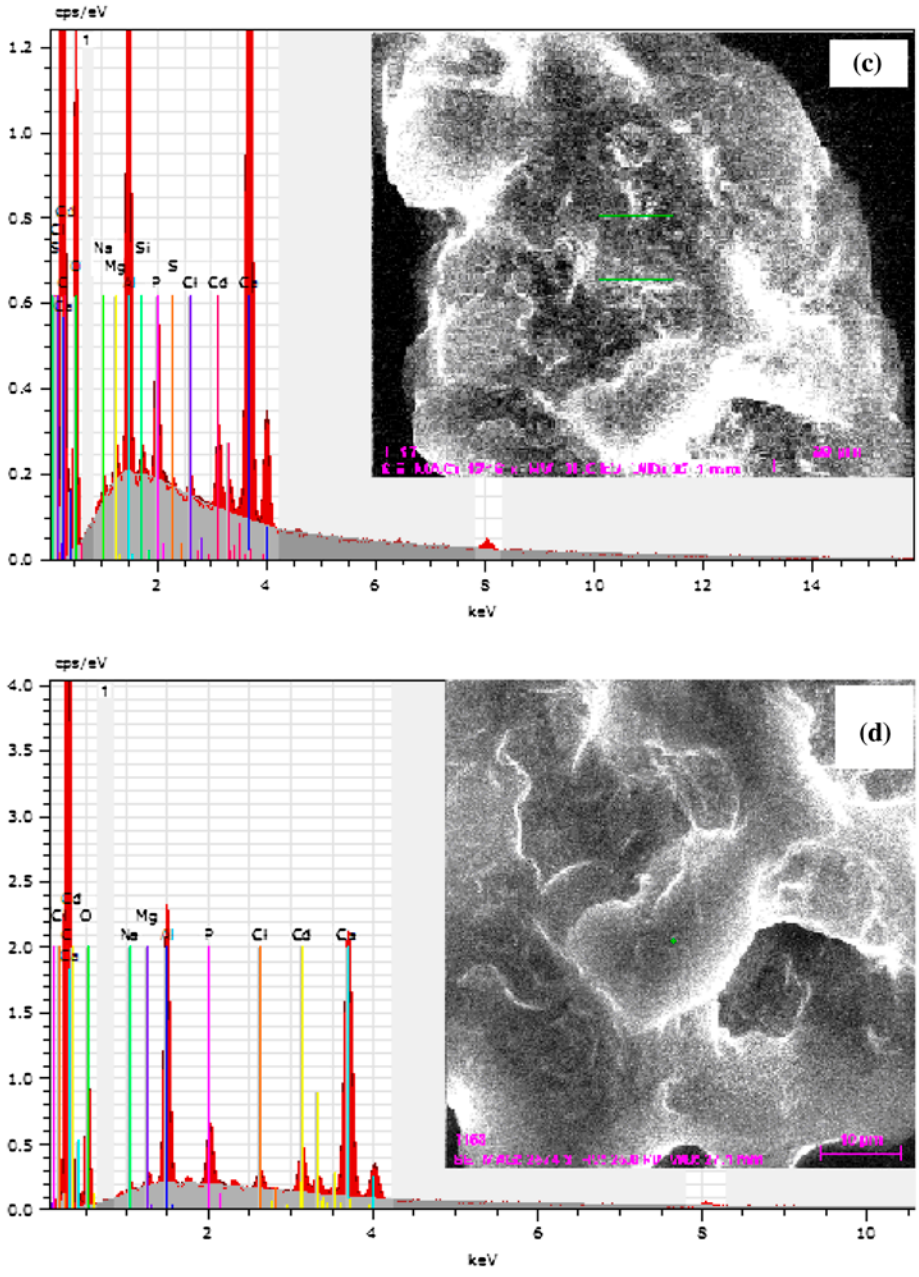

Fig. 8. (*Continued*)

groups in Cd (II) binding by the bacterial biomass. A previous report on extended x-ray absorption fine structure analysis of the Cd (II) bound to the *B. subtilis* cell wall indicated that sequestered Cd (II) is coordinated by phosphoryl groups in a monodentate mode and by carboxyl groups in a bidentate fashion [24].

3.5. ESEM-EDX analyses

The biomass surface, before and after Cd (II) exposure, was characterized using ESEM-EDX. The SEM result in Fig. 8 shows that the images of biomass loaded with Cd (II) were markedly different from those free of Cd (II), indicating that the Cd (II) adsorption induced substantial modifications on the biomass surface.

Conclusive identification of the element was achieved by EDX microanalysis (Fig. 8). Compared to the Cd-free control sample, the presence of specific peaks for Cd in Cd-loaded sample confirmed the Cd accumulation on the biomass. The EDX spectrum of the biomass before metal uptake (Fig. 8(a) and (b)) exhibited distinct peaks of C, O, Al, Ca, P, Cl, Na, Mg, S, and Si, indicating the presence of these elements in the

biomass. Following Cd (II) uptake, the spectra (Fig. 8(c) and (d)) showed peaks not only for Cd, but also for the elements mentioned. Moreover, relative abundance values of Na, Mg, and Ca obtained from the microanalysis of elements present in the Cd-exposed sample were not significantly different compared to the unexposed (control) biomass. These results suggest that Cd (II) adsorption onto biomass was not principally by ion-exchange process. Unlike the observations of Wang et al. [18], adsorption of Cu (II) ions from aqueous solution using *Sphingomonas paucimobilis* biomass was mainly by ion-exchange process.

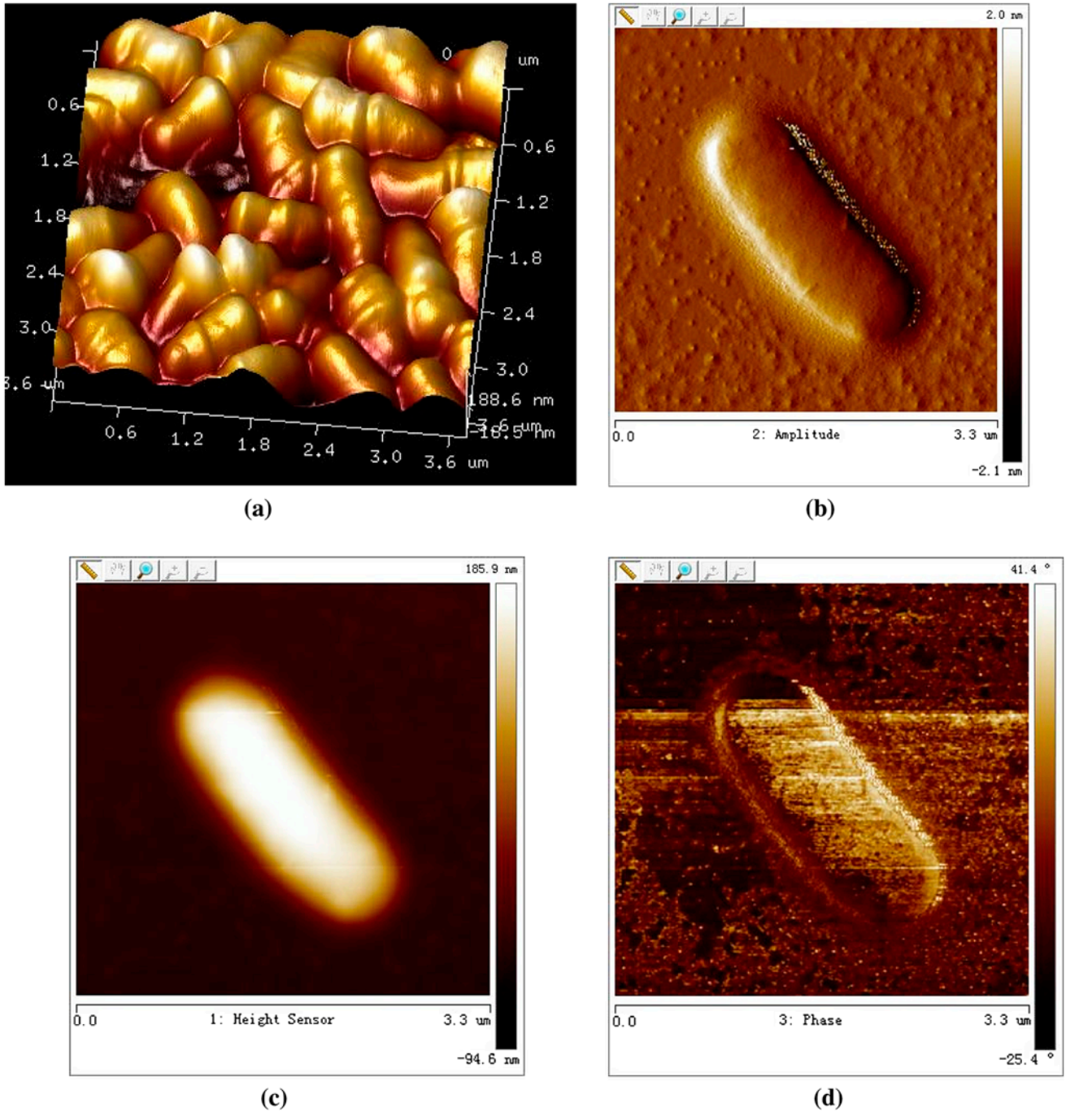

Fig. 9. AFM microscopic images of bacterial cells before Cd (II) exposure (a: three-dimensional image, b: amplitude image; c: height image; d: phase image).

3.6. AFM analyses

The AFM is an ideal tool for determining changes in cellular morphology [17]. In the present study, AFM was used to investigate the bacterial cell surface morphology following Cd (II) uptake. (Figs. 9 and 10) present the morphological comparison among the cells before and after Cd exposure. Our results indicate that adsorption of Cd (II) onto biomass induced substantial modification on cell surfaces. This modification is likely ascribed to the fact that the interaction of Cd (II) with surface functional groups leads to a change in surface architecture as reflected by an increase in

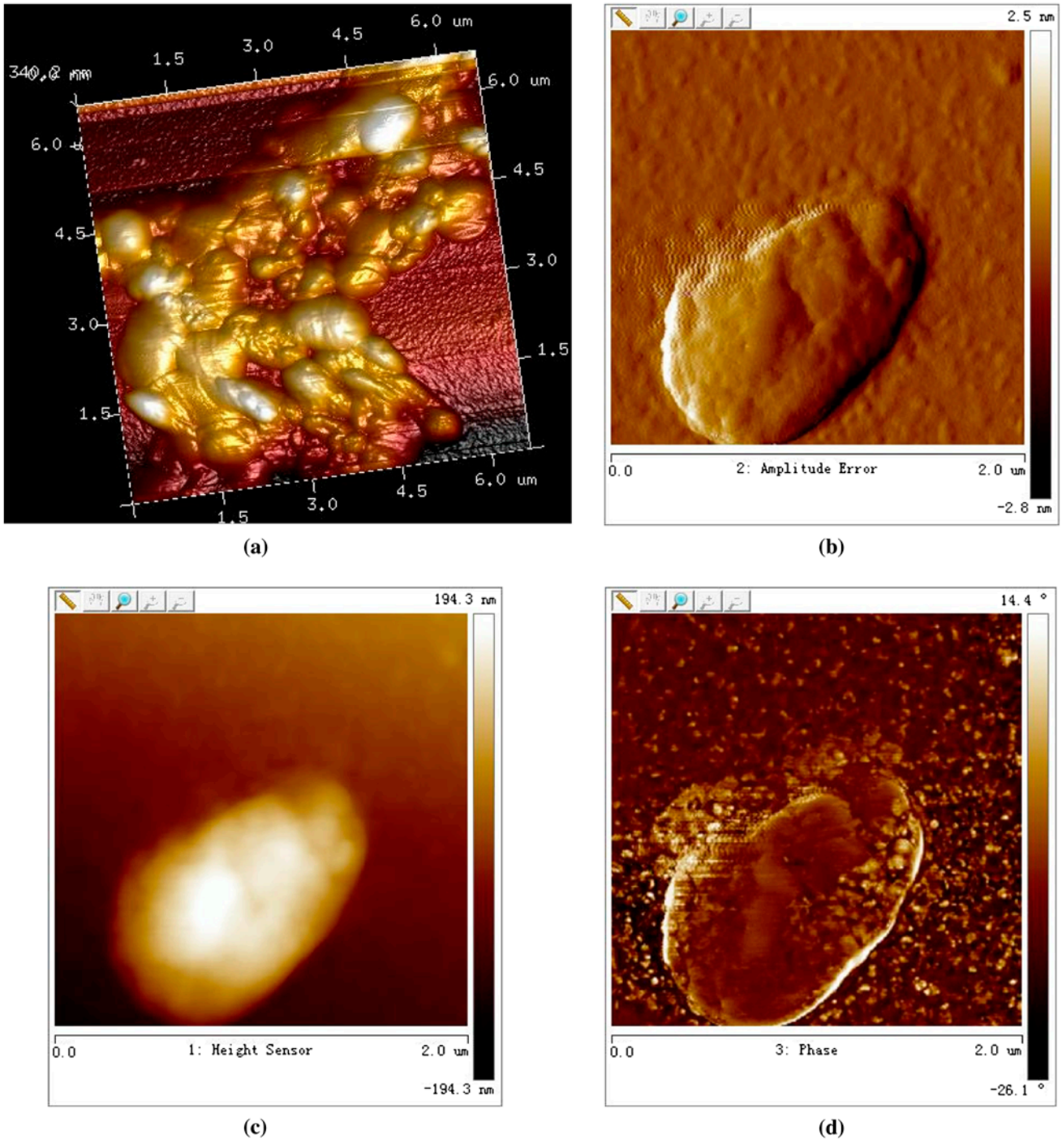

Fig. 10. AFM microscopic images of bacterial cells loaded with Cd (II) (a: three-dimensional image, b: amplitude image; c: height image; d: phase image).

surface roughness or irregularity. Similar results were reported by Chen and Wang [25], who studied the cell surface characteristics of *Saccharomyces cerevisiae* after Pb (II) uptake by AFM.

4. Conclusions

In this study, the adsorption of Cd (II) on to *A. protophormiae* biomass from aqueous solutions was investigated in batch experimental system. The solution pH played a significant role in influencing the Cd (II) adsorption. The Cd (II) adsorption was very rapid and the kinetic data conformed to the pseudo-first -order equation. The isothermal experimental data were fitted by Langmuir and Freundlich isotherms very well. Involvement of cellular phosphate and carboxyl functional groups in Cd (II) binding was evident from FTIR spectroscopy. The AFM showed substantial modification of bacterial cells following Cd (II) adsorption. *A. protophormiae* biomass is an attractive system for possible use in Cd (II) removal and recovery applications.

Acknowledgments

The author acknowledges the work of three anonymous reviewers whose comments and suggestions greatly improved the quality of this manuscript. The material is based upon work supported by Open-end Funds of Jiangsu Key Laboratory of Marine Biotechnology, Huaihai Institute of Technology (2011HS004) and Jiangsu Students' Training Project (2012JSSPITP2602).

References

[1] J. Godt, F. Scheidig, C. Grosse-Siestrup, V. Esche, P. Brandenburg, A. Reich, D.A. Groneberg, The toxicity of cadmium and resulting hazards for human health, J. Occup. Med. Toxicol. 1 (2006) 22–24.
[2] K.S. Rao, M. Mohapatra, S. Anand, P. Venkateswarlu, Review on cadmium removal from aqueous solutions, Int. J. Eng. Sci. Technol. 2 (2010) 81–103.
[3] W.A. Rickelton, The removal of cadmium impurities from cobalt–nickel solutions by precipitation with sodium diisobutyldithiophosphinate, Hydrometallurgy 50 (1998) 339–344.
[4] Y. Ku, M.H. Wu, Y.S. Shen, A study on the cadmium removal from aqueous solutions by zinc cementation, Sep. Sci. Technol. 37 (2002) 571–590.
[5] S. Ahmed, S. Chughtai, M.A. Keane, The removal of cadmium and lead from aqueous solution by ion exchange with Na-Y zeolites, Sep. Purif. Technol. 13 (1998) 57–64.
[6] B. Swain, K. Sarangi, R.P. Das, Effect of different anions on separation of cadmium and zinc by supported liquid membrane using TOPS-99 as mobile carrier, J. Membr. Sci. 277 (2006) 240–248.
[7] B.R. Reddy, D.N. Priya, K.H. Park, Separation and recovery of cadmium(II), cobalt(II) and nickel(II) from sulphate leach liquors of spent Ni-Cd batteries using phosphorus based extractants, Sep. Purif. Technol. 50 (2006) 161–166.
[8] X.S. Wang, Z.P. Lu, H.H. Miao, W. He, H.L. Shen, Kinetics of Pb (II) adsorption on black carbon derived from wheat residue, Chem. Eng. J. 166 (2011) 986–993.
[9] X.S. Wang, H.H. Miao, W. He, H.L. Shen, Competitive adsorption of Pb (II), Cu (II) and Cd (II) ions on wheat-residue derived black carbon, J. Chem. Eng. Data 56 (2011) 444–449.
[10] J. Wang, C. Chen, Biosorbents for heavy metals removal and their future, Biotechnol. Adv. 27 (2009) 195–226.
[11] K. Vijayaraghavan, Y.S. Yun, Bacterial biosorbents and biosorption, Biotechnol. Adv. 26 (2008) 266–291.
[12] E.I. Yilmaz, N.Y. Ensari, Cadmium biosorption by *Bacillus circulans* strain EB1, World J Microbiol. Biotechnol. 21 (2005) 777–779.
[13] W.B. Lu, J.J. Shi, C.H. Wang, J.S. Chang, Biosorption of lead, copper and cadmium by an indigenous isolate *Enterobacter* sp. J1 possessing high heavy-metal resistance, J. Hazard. Mater. 134 (2006) 80–86.
[14] R. Pardo, M. Herguedas, E. Barrado, M. Vega, Biosorption of cadmium, copper, lead and zinc by inactive biomass of *Pseudomonas putida*, Anal. Bioanal. Chem. 376 (2003) 26–32.
[15] P.R. Puranik, N.S. Chabukswar, K.M. Paknikar, Cadmium biosorption by *Streptomyces pimprina* waste biomass, Appl. Microbiol. Biotechnol. 43 (1995) 1118–1121.
[16] L.E. He, B.M. Tebo, Surface charge properties of and Cu(II) adsorption by spores of the marine *Bacillus* sp. strain SG-1, Appl. Environ. Microbiol. 64 (1998) 1123–1129.
[17] S.K. Kazy, S.F. D'Souza, P. Sar, Uranium and thorium sequestration by a *Pseudomonas* sp.: Mechanism and chemical characterization, J. Hazard. Mater. 163 (2009) 65–72.
[18] X.S. Wang, L.P. Huang, Y. Li, J. Chen, Removal of Cu (II) using *Sphingomonas paucimobilis* biomass from aqueous solutions, Adsorpt. Sci. Technol. 28 (2010) 137–147.
[19] QY Zhou, Microbiology of Environmental Engineering, Higher Education Press, Beijing, 1998.
[20] Y.S. Ho, G. McKay, The kinetics of sorption of divalent metal ions onto sphagnum moss peat, Water Res. 34 (2000) 735–742.
[21] Y. Muñoz-González, R. Arriagada-Acuña, G. Soto-Garrido, R. García-Lovera, Activated carbons from peach stones and pine sawdust by phosphoric acid activation used in clarification and decolorization processes, J. Chem. Technol. Biotechnol. 84 (2009) 39–47.
[22] J. Schmitt, H.C. Flemming, FTIR-spectroscopy in microbial and material analysis, Int. Biodeterior. Biodegrad. 41 (1998) 1–11.
[23] L. Svecova, M. Spanelova, M. Kubal, E. Guibal, Cadmium lead and mercury biosorption on waste fungal biomass issued from fermentation industry I Equilibrium studies, Sep. Purif. Technol. 52 (2006) 142–153.
[24] K.M. Kemner, E.J. O'Loughlin, S.D. Kelly, M.I. Boyanov, Synchrotron X-ray investigations of mineral-microbe-metal interactions, Elements 1 (2005) 217–221.
[25] C. Chen, J.L. Wang, Cell surface characteristics of *Saccharomyces cerevisiae* after Pb (II) uptake, Acta Sci. Circumst. 31 (2011) 1587–1593, (in chinese).